A Two-Stage Robust Optimization for Centralized-Optimal Dispatch of Photovoltaic Inverters in Active Distribution Networks

Ding, Tao; Li, Cheng; Yang, Yongheng; Jiang, Jiangfeng; Bie, Zhaohong; Blaabjerg, Frede

Published in:
IEEE Transactions on Sustainable Energy

DOI (link to publication from Publisher):
10.1109/TSTE.2016.2605926

Publication date:
2017

This article has been accepted for publication in a future issue of this journal, but has not been fully edited. Content may change prior to final publication. Citation information: DOI 10.1109/TSTE.2016.2605926, IEEE Transactions on Sustainable Energy

A Two-Stage Robust Optimization for Centralized-Optimal Dispatch of Photovoltaic Inverters in Active Distribution Networks

Tao Ding, *Member, IEEE*, Cheng Li, *Student Member, IEEE*, Yongheng Yang, *Member, IEEE*, Jiangfeng Jiang, *Student Member, IEEE*, Zhaohong Bie, *Senior Member, IEEE*, Frede Blaabjerg, *Fellow, IEEE*

***Abstract*—Optimally dispatching Photovoltaic (PV) inverters is an efficient way to avoid overvoltage in active distribution networks, which may occur in the case of PV generation surplus load demand. Typically, the dispatching optimization objective is to identify critical PV inverters that have the most significant impact on the network voltage level. Following, it ensures the optimal set-points of both active power and reactive power for the selected inverters, guaranteeing the entire system operating constraints (e.g., the network voltage magnitude) within reasonable ranges. However, the intermittent nature of solar PV energy may affect the selection of the critical PV inverters and also the final optimal objective value. In order to address this issue, a two-stage robust centralized-optimal dispatch model is proposed in this paper to achieve a robust PV inverter dispatch solution considering the PV output uncertainties. In addition, the conic relaxation-based branch flow formulation and the column-and-constraint generation (CCG) algorithm are employed to deal with the proposed robust optimization model. Case studies on a 33-bus distribution network and comparisons with the deterministic optimization approach have demonstrated the effectiveness of the proposed method.**

***Index Terms*—Two-stage robust optimization; optimal inverter dispatch (OID); column-and-constraint generation algorithm; active distribution network; photovoltaic generation**

NOMENCLATURE

Parameters

B	Set of buses
E	Set of branches
V	Set of buses without installed PV systems
J	Set of buses with installed PV systems
$\|J\|$	Cardinality of J
r_{ij}, x_{ij}	Resistance/reactance of branch (i, j)
$b_{s,j}$	Shunt susceptance from j to ground
$\pi(j)$	Set of all parents of the bus j
$\delta(j)$	Set of all children of the bus j
$P_{L,j}$, $Q_{L,j}$	Load active and reactive power of PV system j
$P_{s,j}^{f}$	Forecasted active power from PV system j
S_j	Rated apparent power of PV system j
θ_j	Power factor angel of PV system j
$U_j^{\max}$,$U_j^{\min}$	Maximum/ Minimum limit of voltage magnitude at the bus j
$I_{ij}^{\max}$	Limit of current magnitude on branch (i, j)
$P_{s,j}^{\min}$, $P_{s,j}^{\max}$	Lower/upper bound of the forecasted active power from PV system j
ρ	Price of real power losses
a_j	Price of curtailed real power of PV system j
K	Budget factor of PV inverters for ancillary services

Variables

H_{ij}, G_{ij}	Active/reactive power flow from the bus i to j
U_j	Voltage magnitude of bus j
$P_{s,j}$, $Q_{s,j}$	Active and reactive power from photovoltaic system j
u_j	Squared voltage magnitude of bus j
l_{ij}	Squared current magnitude of branch (i, j)
z_j	Binary variable indicating whether photovoltaic inverter j provides ancillary services;

This work was supported in part by the National Natural Science Foundation of China (Grant 51607137), in part by the China Postdoctoral Science Foundation (2015M580847), in part by the Natural Science Basis Research Plan in Shaanxi Province of China (2016JQ5015), in part by the project of State Key Laboratory of Electrical Insulation and Power Equipment in Xi'an Jiaotong University (EIPE16301) and in part by the National Key Basic Research Program of China (2016YFB0901904).

T. Ding (e-mail: tding15@mail.xjtu.edu.cn), C. Li, J. Jiang and Z. Bie are with the State Key Laboratory of Electrical Insulation and Power Equipment, Department of Electrical Engineering, Xi'an Jiaotong University, Xi'an, Shaanxi, 710049, China;

Y. Yang and F. Blaabjerg are with the Department of Energy Technology, Aalborg University, Aalborg DK-9220, Denmark (e-mail: yoy@et.aau.dk; fbl@et.aau.dk).

I. INTRODUCTION

Concerns on environmental conditions have become more critical, which enables an increasing utilization of solar energies [1]-[4]. The Photovoltaic (PV) generation, as a renewable energy, accounts for more than 6% of global energy generation in 2014 because of its continuously declining cost [5]. However, the high penetration of PV systems has challenged the operation and control of grid-connected low-voltage distribution networks [6]-[13]. Thus, solutions to those challenging issues are also observed in literature. In [6] and [7], combining energy storage and PV generation to facilitate scalable plants was studied. It was [8] and [9] that investigated the power quality issues of PV power plants, such as voltage dips and supply interruptions. While [10]-[13] focused on the study of the current harmonic distortion from PV-inverter integration.

In practice, another challenge is associated with overvoltage issue experienced during periods when the total PV generation exceeds the total load demand [14]-[16]. To address this problem, efforts to upgrade inverter controls and advance the existing models for providing ancillary services have been devoted into in such a way that the reliability of electrical power system is attained [17]-[23]. Commonly, these ancillary

This article has been accepted for publication in a future issue of this journal, but has not been fully edited. Content may change prior to final publication. Citation information: DOI 10.1109/TSTE.2016.2605926, IEEE Transactions on Sustainable Energy

services include Reactive Power Control (RPC) methods [17]-[18], Active Power Curtailment (APC) approaches [19]-[20], Optimal Inverter Dispatch (OID) strategies [21]-[23], and so on.

For RPC, absorbing or supplying reactive power based on monitoring electrical quantities of a specific area has been recognized as a feasible solution to effective voltage regulation. However, the voltage regulation with reactive power control may come at the cost of low power factor at feeders and high network current, which will thus cause additional power losses and even overheating (e.g., transformers). Alternatively, APC approaches, only effective in low-voltage distribution systems with high resistance-to-inductance ratios (i.e., large R/X), rely on operating inverters at unity power factor, while curtailing a part of the available active power. However, it will decrease the capacity of installed PV active power and make voltage magnitudes more sensitive to variations of the active power output, especially in the case of PV systems of high intermittency. Furthermore, OID strategies are proposed in [21]-[23] to identify critical PV inverters that have the most significant impact on the network performance. Then, the optimal set-points of active power and reactive power of the corresponding inverters can be scheduled, ensuring the voltage regulation. Actually, the OID takes the advantages of both RPC and APC. Hence, the OID methods are of high effectiveness in such applications. Yet, the forecasting uncertainties of PV systems may affect the optimal selection of the critical PV converters for providing ancillary services, since the PV power generation is highly dependent on the environmental conditions [24]-[25]. However, this challenge to the OID strategy remains unaddressed.

In order to deal with these uncertainties, the probabilistic and stochastic programming was widely used [26]-[29]. For instance, in [26], the availability of dispatchable energy storage and PV generation in micro-grids were studied by modeling the stochastic variables computation through their probability distribution functions. In [27], a stochastic optimal voltage control strategy considering irradiance forecast errors was proposed, where the probability distribution-based stochastic operational risks were defined through chance constraints. Furthermore, a distributed control and generation estimation approach was developed in [28] to coordinate multiple PV systems using stochastic adjacency matrix. In [29], a search-based optimization method was presented to determine optimal sizing and reliability analysis of a hybrid power system including the renewable resources and energy storage systems considering the probability distribution function of the stochastic renewable resource generation.

Nevertheless, it is usually difficult to obtain the accurate probability distribution function of uncertainties. State-of-the-art robust optimization methods become more and more popular in power system research, due to the effectiveness in achieving robust operation in the presence of uncertainties, since these approaches have lots of advantages: a) an exact hard-to-obtain probability distribution is not required, which facilitates the modeling of uncertainties [30]; b) the robust optimization model constructs an optimal solution that immunizes against all realizations governed by the uncertainty set, instead of seeking the solution in the probabilistic sense to stochastic uncertainty [31]; c) the computational tractability is also a primary motivation and goal [32]. It should be noted that the traditional robust optimization models for power system applications in [30]-[32] were based on the DC power flow. It is urgent to study the AC power flow based robust optimization, especially for the distribution networks, since the voltage magnitude should be strictly considered.

In light of the above issues, this paper proposes a robust two-stage optimization model to resolve those challenges. Major contributions are summarized as

- A two-stage robust optimization model is set up for the centralized-optimal dispatch of PV inverters in active distribution networks, considering PV output uncertainties.
- A general second-order cone programming (SOCP) based column-and-constraint generation (CCG) algorithm is proposed to solve the two-stage robust optimization model in active distribution networks.

The rest of the paper is organized as follows. Section II presents the general mathematical formulation of the OID model and the conic relaxation method. In Section III, a two-stage robust optimization model is set up for the OID model with the consideration of uncertainties in PV power generation and a column-and-constraint generation algorithm is proposed to solve the proposed model. Numeric results on a 33-bus distribution network are presented in Section VI to illustrate the effectiveness of the proposed method. Finally, conclusions are drawn in Section V.

II. Optimal Dispatch Model of PV Inverters

A. Distribution Network Model Using Branch Flow Form

It was proposed in [33] that the branch flow formulation was widely used in radial networks to describe the power flow. As shown in Fig. 1, the branch flow formulation actually reflects the Kirchhoff's law of the network. For a radial network with n+1 buses and n branches, we have

$$\begin{cases} P_{s,j}-P_{L,j}=\sum\limits_{k\in\delta(j)}H_{jk}-\sum\limits_{i\in\pi(j)}\left(H_{ij}-r_{ij}\dfrac{H_{ij}^2+G_{ij}^2}{U_i^2}\right),\ \forall j\in B \\ Q_{s,j}-Q_{L,j}=\sum\limits_{k\in\delta(j)}G_{jk}-\sum\limits_{i\in\pi(j)}\left(G_{ij}-x_{ij}\dfrac{H_{ij}^2+G_{ij}^2}{U_i^2}\right)+b_{s,j}U_j^2,\ \forall j\in B \\ U_j^2=U_i^2-2\left(r_{ij}H_{ij}+x_{ij}G_{ij}\right)+\left(r_{ij}^2+x_{ij}^2\right)\dfrac{H_{ij}^2+G_{ij}^2}{U_i^2},\ \forall(i,j)\in E \end{cases} \quad (1)$$

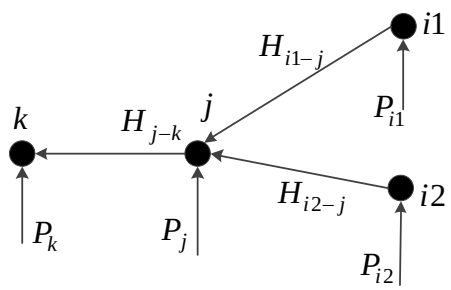

Fig. 1. A simple radial network with active power flow.

Specifically, the load model is adopted by a constant PQ model, and for given solar irradiation conditions, the maximum

This article has been accepted for publication in a future issue of this journal, but has not been fully edited. Content may change prior to final publication. Citation information: DOI 10.1109/TSTE.2016.2605926, IEEE Transactions on Sustainable Energy

available active power from the *j*-th PV unit is $P_{s,j}^{\max}$. Nevertheless, it has been presented in [21]-[23] that the PV inverters are allowed providing ancillary grid services by curtailing their active power outputs to meet the operation constraints of the distribution networks, such as voltage magnitude limits, current limits, etc.. Certainly, if the *j*-th PV inverter is chosen to provide ancillary services, it will receive the corresponding reward and its operating space in the *PQ* plane is given by

$$F_j\left(z_j=1\right)=\left\{\left(P_{s,j},Q_{s,j}\right)\left|\begin{array}{c} Q_{s,j}^2+P_{s,j}^2\le S_j^2 \\ 0\le P_{s,j}\le P_{s,j}^f \\ -\tan\theta_j\left(P_{s,j}\right)\le Q_{s,j}\le\tan\theta_j\left(P_{s,j}\right)\end{array}\right.\right\} \tag{2}$$

On the other hand, if the *j*-th PV inverter is not chosen to provide ancillary services, its operating state is given by

$$F_j^{OID}\left(z_j=0\right)=\left\{\left(P_{s,j},Q_{s,j}\right)\middle|P_{s,j}=P_{s,j}^f,\ \ Q_{s,j}=0\right\} \tag{3}$$

As shown in Fig. 2, the OID strategy allows adjusting both active and reactive powers, which gives the largest operating regions compared to other strategies. Moreover, it can be found that if the PV inverter is chosen to provide ancillary services, the reactive power capability is limited by the inverter rating (i.e., the apparent power and power factor angle), which is given by (2).

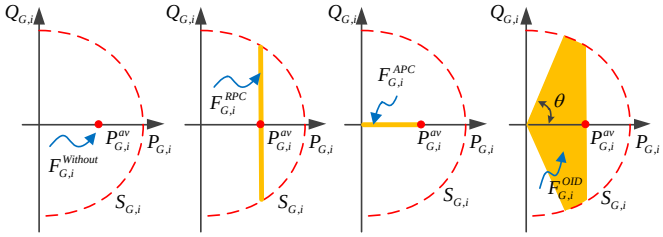

Fig. 2. Operating regions for the PV inverters for different strategies: (a) without the ancillary services, (b) with the RPC, (c) with the APC, and (d) with the OID strategy.

Furthermore, with an increase in the PV penetration, either the current or the total network losses will increase, and thus the efficiency of the PV active power may decrease. As a result, the optimal dispatch model of PV inverters in this paper aims to maximize the total real power surplus (i.e., total PV generation minus network losses), by selecting the subset of critical PV inverters and finding the real and reactive power operating points, while considering various equality and inequality constraints in relation to the power balance and network security. For instance, voltage magnitudes and branch currents should be within their reasonable ranges.

Besides, it can be found in (1) that the expression $\frac{H_{ij}^2+G_{ij}^2}{U_i^2}$ is just the squared current magnitude of the branch *ij*, so we have $l_{ij}=\frac{H_{ij}^2+G_{ij}^2}{U_i^2}$. Furthermore, the optimization model can be exactly written as

$$\max_{\{P_{s,h},Q_{s,h},z_h,U_j,G_{ij},H_{ij}\}}\ \ \sum_{j\in J}P_{s,j}-\sum_{(i,j)\in E}r_{ij}l_{ij} \tag{4-a}$$

$$\Leftrightarrow\ \min_{\{P_{s,h},Q_{s,h},z_h,U_j,G_{ij},H_{ij}\}}\ \ \sum_{(i,j)\in E}r_{ij}l_{ij}-\sum_{j\in J}P_{s,j} \tag{4-b}$$

$$s.t.\ \ P_{s,j}^f-P_{L,j}=\sum_{k\in\delta(j)}H_{jk}-\sum_{i\in\pi(j)}\left(H_{ij}-r_{ij}l_{ij}\right),\ \forall j\in V\setminus J \tag{5}$$

$$-Q_{L,j}=\sum_{k\in\delta(j)}G_{jk}-\sum_{i\in\pi(j)}\left(G_{ij}-x_{ij}l_{ij}\right)+b_{s,j}U_j^2,\ \forall j\in V\setminus J \tag{6}$$

$$P_{s,j}-P_{L,j}=\sum_{k\in\delta(j)}H_{jk}-\sum_{i\in\pi(j)}\left(H_{ij}-r_{ij}l_{ij}\right),\ \forall j\in J \tag{7}$$

$$Q_{s,j}-Q_{L,j}=\sum_{k\in\delta(j)}G_{jk}-\sum_{i\in\pi(j)}\left(G_{ij}-x_{ij}l_{ij}\right)+b_{s,j}U_j^2,\ \forall j\in J \tag{8}$$

$$-P_{L,j}=\sum_{k\in\delta(j)}H_{jk}-\sum_{i\in\pi(j)}\left(H_{ij}-r_{ij}l_{ij}\right),\ \forall j\in B\setminus V \tag{9}$$

$$-Q_{L,j}=\sum_{k\in\delta(j)}G_{jk}-\sum_{i\in\pi(j)}\left(G_{ij}-x_{ij}l_{ij}\right)+b_{s,j}U_j^2,\ \forall j\in B\setminus V \tag{10}$$

$$U_j^2=U_i^2-2\left(r_{ij}H_{ij}+x_{ij}G_{ij}\right)+\left(r_{ij}^2+x_{ij}^2\right)l_{ij},\ \forall(i,j)\in E \tag{11}$$

$$U_j^{\min}\le U_j\le U_j^{\max},\quad \forall j\in B \tag{12}$$

$$0\le l_{ij}\le\left(I_{ij}^{\max}\right)^2,\quad \forall(i,j)\in E \tag{13}$$

$$P_{s,j}^f\left(1-z_j\right)\le P_{s,j}\le P_{s,j}^f,\qquad \forall j\in J \tag{14}$$

$$\left\|\begin{matrix}Q_{s,j}\\P_{s,j}z_j\end{matrix}\right\|_2\le S_j,\qquad \forall j\in J \tag{15}$$

$$-z_jP_{s,j}\tan\theta_j\le Q_{s,j}\le z_jP_{s,j}\tan\theta_j,\qquad \forall j\in J \tag{16}$$

$$H_{ij}^2+G_{ij}^2=l_{ij}U_i^2,\qquad \forall(i,j)\in E \tag{17}$$

$$z_j\in\{0,1\}^{|H|},\quad \sum_{j\in J}z_j\le K \tag{18}$$

where the objective function (4-a) is to maximize the total PV generation minus network losses and it equals to minimize the network losses minus the total PV generation, i.e., the objective function (4-b); equations (5)-(11) are the branch flow model from (1); constraints (12)-(13) refer to nodal voltage magnitude and branch current limits; (14)-(16) denote the operating region of each PV inverter: if the *j*-th PV inverter is chosen to provide ancillary services (i.e., z_j=1), the operating region is (2) and if the *j*-th PV inverter will not provide ancillary services (i.e., z_j=0), the operating region is (3); constraint (17) refers to the expression of the branch current; constraint (18) offers the budget of PV inverters for ancillary services, i.e., to choose the given number of controlled inverters considering the net operational cost of the residential feeders [21].

B. Conic Relaxation and Mixed Integer Second Order Cone Programming Based Optimal Dispatch of PV Inverters

Technically, the OID strategies in (4)-(18) can be formulated as a mixed integer nonconvex programming (MINNP) model due to the nonconvex feasible region enclosed by the power flow equations. Referring to the state-of-the-art conic relaxation techniques, the non-convex power flow equations (1) can be relaxed using second-order cones. Thus, the model in (4)-(18) can be transformed into a mixed integer convex programming that can be tractably solved by commercial solvers, in contrast to the original mixed integer non-convex programming.

This article has been accepted for publication in a future issue of this journal, but has not been fully edited. Content may change prior to final publication. Citation information: DOI 10.1109/TSTE.2016.2605926, IEEE Transactions on Sustainable Energy

Firstly, a transformation given by (19) aims to utilize a new variable u_j to replace U_j^2 in the model of (4)-(18).

$$U_j^2 = u_j \quad \forall j \in B \tag{19}$$

Thus, the nonlinear terms in the constraints of (6), (8), (10) and (11) induced by U_j^2 will be eliminated, which leads to affine equalities as

$$-Q_{L,j} = \sum_{k\in\delta(j)} G_{jk} - \sum_{i\in\pi(j)} \left(G_{ij} - x_{ij} l_{ij}\right) + b_{s,j} u_j , \qquad \forall j \in V \setminus J \tag{20}$$

$$Q_{s,j} - Q_{L,j} = \sum_{k\in\delta(j)} G_{jk} - \sum_{i\in\pi(j)} \left(G_{ij} - x_{ij} l_{ij}\right) + b_{s,j} u_j , \forall j \in J \tag{21}$$

$$-Q_{L,j} = \sum_{k\in\delta(j)} G_{jk} - \sum_{i\in\pi(j)} \left(G_{ij} - x_{ij} l_{ij}\right) + b_{s,j} u_j , \forall j \in B \setminus V \tag{22}$$

$$u_j = u_i - 2\left(r_{ij} H_{ij} + x_{ij} G_{ij}\right) + \left(r_{ij}^2 + x_{ij}^2\right) l_{ij} , \forall (i,j) \in E \tag{23}$$

Moreover, it should be noted that after the reformulation using u_j, the variable U_j will not appear in any constraint except for (12). Since the square of the voltage magnitude is always positive, taking the square of (12) gives

$$\left(U_j^{\min}\right)^2 \le U_j^2 \le \left(U_j^{\max}\right)^2 \xrightarrow{U_j^2 = u_j} \left(U_j^{\min}\right)^2 \le u_j \le \left(U_j^{\max}\right)^2 , \quad \forall j \in B \tag{24}$$

Secondly, after the above reformulation, the nonconvex property only exists in the quadratic equalities of (17). To address this problem, the conic relaxation techniques are utilized to relax (17) into inequalities. Thus, it gives

$$H_{ij}^2 + G_{ij}^2 \le l_{ij} u_i , \quad \forall (i,j) \in E \tag{25}$$

Mathematically, (20) can be reformulated as a standard second-order cone formulation:

$$\left\| \begin{matrix} 2H_{ij} \\ 2G_{ij} \\ l_{ij} - u_i \end{matrix} \right\|_2 \le l_{ij} + u_i , \quad \forall (i,j) \in E \tag{26}$$

Additionally, it can be observed in (15) and (16) that there are bilinear terms $z_j P_{s,j}$, which are non-convex. Fortunately, these bilinear terms are formed by one continuous variable multiplying one binary variable, which can be exactly reformulated using the Big M approach [34]-[35] as follows:

$$z_j P_{s,j} = \begin{cases} P_{s,j} & \text{if } z_j = 1 \\ 0 & \text{if } z_j = 0 \end{cases} \Leftrightarrow \begin{cases} -M z_j \le T_{s,j} \le M z_j \\ -M\left(1 - z_j\right) + P_{s,j} \le T_{s,j} \le P_{s,j} + M\left(1 - z_j\right) \end{cases} \tag{27}$$

where M is a large number and $T_{s,j}$ is a dummy variable.

According to the above transformations, the original optimization model (4)-(18) is relaxed into a 0-1 mixed integer second-order cone programming as follows:

$$\min_{\{P_{s,h}, Q_{s,h}, z_h, u_j, l_{ij}, G_{ij}, H_{ij}\}} \sum_{(i,j)\in E} r_{ij} l_{ij} - \sum_{j\in J} P_{s,j} \tag{28}$$

$$s.t. \quad (5), (7), (9), (13)\text{-}(14), (18), (20)\text{-}(23), (24), (26) \tag{29}$$

$$\left\| \begin{matrix} Q_{s,j} \\ T_{s,j} \end{matrix} \right\|_2 \le S_j , \qquad \forall j \in J \tag{30}$$

$$-T_{s,j} \tan\theta_j \le Q_{s,j} \le T_{s,j} \tan\theta_j , \qquad \forall j \in J \tag{31}$$

$$\begin{cases} -M z_j \le T_{s,j} \le M z_j \\ -M\left(1 - z_j\right) + P_{s,j} \le T_{s,j} \le P_{s,j} + M\left(1 - z_j\right) \end{cases} , \quad \forall j \in J \tag{32}$$

III. Two-Stage Robust Optimization and Column-and-constraint Generation Algorithm

Traditionally, the optimal dispatch model for active power curtailment of PV generation in distribution networks is only conducted under one deterministic snapshot. Considering the uncertainties of PV generation output, the optimal selection of the critical PV converters for providing ancillary services may be different. Thus, a two-stage robust optimization model is set up to select the optimal subset of PV inverters, which is feasible, and thus robust, for any realization of the uncertain PV active power output. Specifically, the first stage variables are binary variables for selecting PV converters, which are served as the "here-and-now" decisions (i.e., they cannot be changed no matter how the uncertainty varies). The second stage variables are continuous variables for dispatching the real and reactive power operating points of PV systems, which are regarded as the "wait-and-see" decisions that can be adjusted with respect to the real PV generation output [36]-[37]. In addition, the two-stage robust optimal dispatch model can be formulated as

$$\min_{\boldsymbol{z}\in Z} 0 + \max_{R_{s,j}\in\Delta} \min_{\{P_{s,h}, Q_{s,h}, z_h, u_j, l_{ij}, G_{ij}, H_{ij}\}} \sum_{(i,j)\in E} r_{ij} l_{ij} - \sum_{j\in J} P_{s,j} \tag{33}$$

$$s.t \quad (29)\text{-}(32) \tag{34}$$

with

$$\Delta = \left\{ P_j \middle| P_{s,j}^{\min} \le R_{s,j} \le P_{s,j}^{\max} , j \in V \right\} \tag{35}$$

$$Z = \left\{ z_j \in \{0,1\}^{|H|} , \forall j \in J; \ \sum_{j\in J} z_j \le K \right\} \tag{36}$$

where Δ is the uncertainty set that denotes the uncertain maximum available PV power output, and Z is the feasible region of the binary variables.

Then, the two-stage robust centralized-optimal dispatch model (33)-(36) can be compactly written as

$$\min_{\boldsymbol{z}} \ \boldsymbol{h}^T \boldsymbol{z} + \max_{\boldsymbol{u}^{\min} \le \boldsymbol{u} \le \boldsymbol{u}^{\max}} \min_{\boldsymbol{y}\in \mathrm{Y}} \ \boldsymbol{a}^T \boldsymbol{y} \tag{37}$$

$$s.t. \qquad \boldsymbol{A}\boldsymbol{z} \ge \boldsymbol{b} , \ \ \boldsymbol{z} \in \{0,1\} \tag{38}$$

$$\mathrm{Y} = \left\{ \begin{matrix} \boldsymbol{y} \middle| \boldsymbol{C}\boldsymbol{y} \le \boldsymbol{f} , \left\| \boldsymbol{Q}_i \boldsymbol{y} + \boldsymbol{q}_i \right\|_2 \le \boldsymbol{c}_i^T \boldsymbol{y} + d_i , i = 1,...,n \\ \boldsymbol{D}\boldsymbol{y} = \boldsymbol{g} - \boldsymbol{G}\boldsymbol{z}, \quad \boldsymbol{E}\boldsymbol{y} = \boldsymbol{u} \end{matrix} \right\} \tag{39}$$

Given the first-stage discrete decision $\boldsymbol{z}^*$, the following sub-problem can be obtained:

$$\max_{\boldsymbol{u}^{\min} \le \boldsymbol{u} \le \boldsymbol{u}^{\max}} \min_{\boldsymbol{y}} \ \boldsymbol{a}^T \boldsymbol{y} \tag{40}$$

$$s.t. \quad \boldsymbol{C}\boldsymbol{y} \le \boldsymbol{f} \tag{41}$$

$$\boldsymbol{D}\boldsymbol{y} = \boldsymbol{g} - \boldsymbol{G}\boldsymbol{z}^* \tag{42}$$

$$\boldsymbol{E}\boldsymbol{y} = \boldsymbol{u} \tag{43}$$

$$\left\| \boldsymbol{Q}_i \boldsymbol{y} + \boldsymbol{q}_i \right\|_2 \le \boldsymbol{c}_i^T \boldsymbol{y} + d_i , \qquad i = 1,...,n \tag{44}$$

Furthermore, the above "max-min" bi-level programming model can be solved using the duality theory for the inner "min" linear programming model, which is equal to a single-level "max" model as

This article has been accepted for publication in a future issue of this journal, but has not been fully edited. Content may change prior to final publication. Citation information: DOI 10.1109/TSTE.2016.2605926, IEEE Transactions on Sustainable Energy

$$\max_{\boldsymbol{\pi}_1,\boldsymbol{\pi}_2,\boldsymbol{\pi}_3,\boldsymbol{u},\lambda_1,\ldots,\lambda_n,\boldsymbol{w}_1,\ldots,\boldsymbol{w}_n} \quad \boldsymbol{f}^T\boldsymbol{\pi}_1+\left(\boldsymbol{g}-\boldsymbol{G}\boldsymbol{z}^*\right)^T\boldsymbol{\pi}_2+\boldsymbol{u}^T\boldsymbol{\pi}_3-\sum_{i=1}^{n}\left(\lambda_i d_i+\boldsymbol{w}_i^T\boldsymbol{q}_i\right) \quad (45)$$

$$s.t. \quad \boldsymbol{C}^T\boldsymbol{\pi}_1+\boldsymbol{D}^T\boldsymbol{\pi}_2+\boldsymbol{E}^T\boldsymbol{\pi}_3+\sum_{i=1}^{n}\left(\boldsymbol{Q}\boldsymbol{w}_i+\lambda_i\boldsymbol{q}_i\right)=\boldsymbol{a} \quad (46)$$

$$\left\|\boldsymbol{w}_i\right\|_2\le\lambda_i, \quad i=1,\ldots,n \quad (47)$$

$$\boldsymbol{\pi}_1\le\boldsymbol{0} \quad (48)$$

$$\boldsymbol{u}^{\min}\le\boldsymbol{u}\le\boldsymbol{u}^{\max} \quad (49)$$

where $\boldsymbol{\pi}_1$, $\boldsymbol{\pi}_2$ and $\boldsymbol{\pi}_3$ are dual variables for the constraints of (41), (42) and (43); (λ_i, $\boldsymbol{w}_i$) is the conic dual variables for the *i*-th second-order cone constraints of (44).

Unfortunately, (45) contains the bilinear terms $\boldsymbol{u}^T\boldsymbol{\pi}_3$ which makes the model nonconvex. To deal with this issue, the bilinear terms can be exactly linearized by further introducing dummy binary variables δ_s. Doing so gives

$$\boldsymbol{u}^T\boldsymbol{\pi}_3=\sum_s u_s\pi_{3,s}=\sum_s\left(u_s^{\min}\pi_{3,s}+\left(u_s^{\max}-u_s^{\min}\right)\pi_{3,s}\delta_s\right) \quad (50)$$

However, there still is a bilinear term $\pi_{3,s}\delta_s$ in (50), but each bilinear term is the product of one continuous variable and one binary variable. Similar to (27), the bilinear terms can be reformulated as

$$\begin{cases}\boldsymbol{u}^T\boldsymbol{\pi}_3=\sum_s u_s\pi_{3,s}=\sum_s\left(u_s^{\min}\pi_{3,s}+\left(u_s^{\max}-u_s^{\min}\right)r_s\right)\\ -M\delta_s\le r_s\le M\delta_s\\ -M\left(1-\delta_s\right)+\pi_{3,s}\le r_s\le\pi_{3,s}+M\left(1-\delta_s\right)\end{cases}, \ \forall s \quad (51)$$

where r_s is a continuous dummy variable. It can be observed that if δ_s=0, the bilinear term $u_s\pi_{3,s}$ leads to u_s=$u_s^{\min}$; if δ_s=1, the bilinear term $u_s\pi_{3,s}$ leads to u_s=$u_s^{\max}$. Thus, we have

$$(\mathbf{SP}) \quad \max_{\boldsymbol{\pi}_1,\boldsymbol{\pi}_2,\boldsymbol{\pi}_3,\boldsymbol{u},\lambda_1,\ldots,\lambda_n,\boldsymbol{w}_1,\ldots,\boldsymbol{w}_n} \quad \begin{aligned}&\boldsymbol{f}^T\boldsymbol{\pi}_1+\left(\boldsymbol{g}-\boldsymbol{G}\boldsymbol{z}^*\right)^T\boldsymbol{\pi}_2-\sum_{i=1}^{n}\left(\lambda_i d_i+\boldsymbol{w}_i^T\boldsymbol{q}_i\right)\\&+\sum_s\left(u_s^{\min}\pi_{3,s}+\left(u_s^{\max}-u_s^{\min}\right)r_s\right)\end{aligned} \quad (52)$$

$$s.t. \quad \boldsymbol{C}^T\boldsymbol{\pi}_1+\boldsymbol{D}^T\boldsymbol{\pi}_2+\boldsymbol{E}^T\boldsymbol{\pi}_3+\sum_{i=1}^{n}\left(\boldsymbol{Q}\boldsymbol{w}_i+\lambda_i\boldsymbol{q}_i\right)=\boldsymbol{a} \quad (53)$$

$$\left\|\boldsymbol{w}_i\right\|_2\le\lambda_i, \quad i=1,\ldots,n \quad (54)$$

$$-M\delta_s\le r_s\le M\delta_s, \quad \forall s \quad (55)$$

$$-M\left(1-\delta_s\right)+\pi_{3,s}\le r_s\le\pi_{3,s}+M\left(1-\delta_s\right), \quad \forall s \quad (56)$$

$$\boldsymbol{\pi}_1\le\boldsymbol{0} \quad (57)$$

$$\boldsymbol{u}^{\min}\le\boldsymbol{u}\le\boldsymbol{u}^{\max} \quad (58)$$

The two-stage robust model has a master-and-sub problem structure, where the Master Problem (MP) tries to find a lower bound of the original model and the Sub Problem (SP) aims to search an upper bound. Then, some cut planes are added into the SP to improve the lower bound, being an iterative process, where the lower bound increases and the upper bound decreases. Finally, the optimal solution is obtained until the gap between the upper and the lower bounds is small enough [38]. Note that the MP and SP models are mixed integer second-order cone programming models that can be tractably handled.

For a given gap ε, the complete procedure of the CCG method for the two-stage robust centralized-optimal dispatch can be described as

Step 1: Let *LB* = –∞, *UB* = +∞, *k* = 0;

Step 2: Solve the (MP) model:

$$(\mathbf{MP}) \quad \min_{\boldsymbol{z},\eta,\boldsymbol{y}^l} \quad \boldsymbol{h}^T\boldsymbol{z}+\eta \quad (59)$$

$$s.t. \quad \boldsymbol{A}\boldsymbol{z}\ge\boldsymbol{b}, \ \boldsymbol{z}\in\{0,1\} \quad (60)$$

$$\eta\ge\boldsymbol{a}^T\boldsymbol{y}^l, \ \forall l\le k \quad (61)$$

$$\left\|\boldsymbol{Q}_i\boldsymbol{y}^l+\boldsymbol{q}_i\right\|_2\le\boldsymbol{c}_i^T\boldsymbol{y}^l+d_i, i=1,\ldots,n, \ \forall l\le k \quad (62)$$

$$\boldsymbol{C}\boldsymbol{y}^l\le\boldsymbol{f}, \ \forall l\le k \quad (63)$$

$$\boldsymbol{D}\boldsymbol{y}^l=\boldsymbol{g}-\boldsymbol{G}\boldsymbol{z}, \ \forall l\le k \quad (64)$$

$$\boldsymbol{E}\boldsymbol{y}^l=\boldsymbol{u}^*, \ \forall l\le k \quad (65)$$

Obtain the optimal solution ($\boldsymbol{z}^*,\eta^*,\boldsymbol{y}^{l*}$) with *l*=1,2,..,*k* and update the lower bound *LB*= η^*;

Step 3: Fix $\boldsymbol{y}^*$ and solve the (SP) in (52)-(58). If the (SP) is feasible, we have ($\boldsymbol{u}^*,\boldsymbol{\pi}_1^*,\boldsymbol{\pi}_2^*,\boldsymbol{\pi}_3^*,\lambda_1^*,\ldots,\lambda_n^*,\boldsymbol{w}_1^*,\ldots,\boldsymbol{w}_n^*$) and the optimal objective value $\vartheta\left(\boldsymbol{z}^*\right)$; otherwise set $\vartheta\left(\boldsymbol{z}^*\right)=+\infty$. Furthermore, update the upper bound as *UB* = min{*UB*, $\vartheta\left(\boldsymbol{y}^*\right)$};

Step 4: If (*UB*–*LB*)≤ε, return $\boldsymbol{y}^*$ and stop. Otherwise, fix $\boldsymbol{u}^*$ and add the cuts as

(a) If the SP in Step 3 is feasible, create variables $\boldsymbol{y}^{l+1}$ and assign the following constraints to MP

$$\eta\ge\boldsymbol{a}^T\boldsymbol{y}^l \quad (66)$$

$$\left\|\boldsymbol{Q}_i\boldsymbol{y}^l+\boldsymbol{q}_i\right\|_2\le\boldsymbol{c}_i^T\boldsymbol{y}^l+d_i, i=1,\ldots,n \quad (67)$$

$$\boldsymbol{C}\boldsymbol{y}^l\le\boldsymbol{f} \quad (68)$$

$$\boldsymbol{D}\boldsymbol{y}^l=\boldsymbol{g}-\boldsymbol{G}\boldsymbol{z} \quad (69)$$

$$\boldsymbol{E}\boldsymbol{y}^l=\boldsymbol{u}^* \quad (70)$$

(b) If the SP in Step 3 is infeasible, create variables $\boldsymbol{y}^{l+1}$ and add the following constraints to MP

$$\left\|\boldsymbol{Q}_i\boldsymbol{y}^l+\boldsymbol{q}_i\right\|_2\le\boldsymbol{c}_i^T\boldsymbol{y}^l+d_i, i=1,\ldots,n \quad (71)$$

$$\boldsymbol{C}\boldsymbol{y}^l\le\boldsymbol{f} \quad (72)$$

$$\boldsymbol{D}\boldsymbol{y}^l=\boldsymbol{g}-\boldsymbol{G}\boldsymbol{z} \quad (73)$$

$$\boldsymbol{E}\boldsymbol{y}^l=\boldsymbol{u}^* \quad (74)$$

Step 5: Update *k*=*k*+1 and go back to Step 2.

IV. Numerical Analysis

A. 33-bus Test System

As shown in Fig. 3, a 33-bus radial distribution network exemplified in [39], was analyzed in this section with the proposed method considering uncertainties in PV power generation. The proposed method was performed in MATLAB with the MOSEK commercial solver.

This article has been accepted for publication in a future issue of this journal, but has not been fully edited. Content may change prior to final publication. Citation information: DOI 10.1109/TSTE.2016.2605926, IEEE Transactions on Sustainable Energy

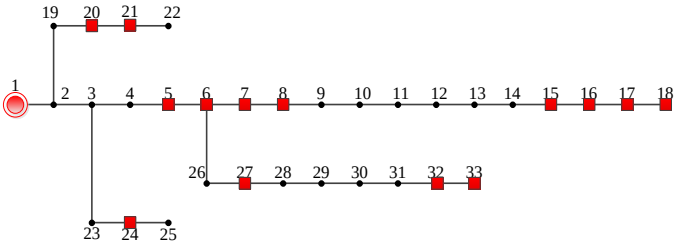

Fig. 3. A 33-bus radial network topology.

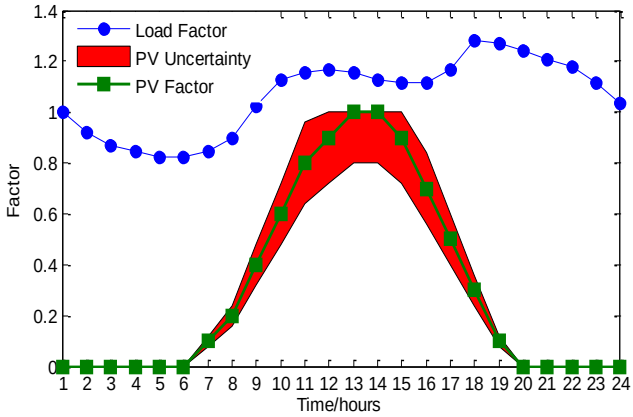

Fig. 4. Load factor and the PV output curve (PV factor) considering the PV system uncertainty.

Here, 14 PV bases are considered and integrated into the 33-bus system with the capacity of each PV base being 300 kW. The uncertainty in PV generation is given by $[(1-\alpha)P_s^f, \min(300, (1+\alpha)P_s^f)]$, where α reflects the confidence interval of the forecasted value. It is obvious that a large α results in large uncertainties in the PV output. Meanwhile, the joint control of active and reactive power proposed in [26] has been adopted, which leads the power factor angle of the PV system to be π/2. In addition, the factor of load and PV output curve is given in Fig. 4, which depicts that the load curve has "double peaks" during 8:00 a.m.~13:00 p.m. and 17:00 a.m.~21:00 p.m., while the PV system generates power only during the daytime 6:00 a.m.~20:00 p.m..

In order to compare the proposed two-stage robust centralized-optimal dispatch approach (denoted as RA) with the traditional Deterministic Approach (DA) by randomly generating 10000 scenarios through the Monte Carlo simulations to find the Worst-Case scenario (WC). Let $\eta = O(\mathrm{RA}) - O(\mathrm{DA})$ denote the error between O(RA) and O(DA), where O(RA) and O(DA) are the results from the RA model and the worst case of the DA model, which includes network losses (η_{Loss}), curtailed active power ($\eta_{\mathrm{Curtailed}}$) and optimal objective value ($\eta_{\mathrm{Objective}}$).

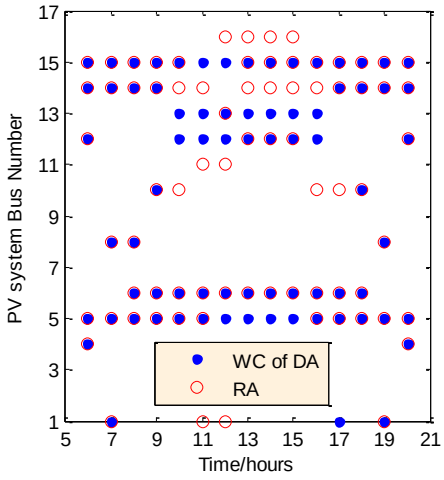

Fig. 5. Optimal selection of PV system for ancillary services.

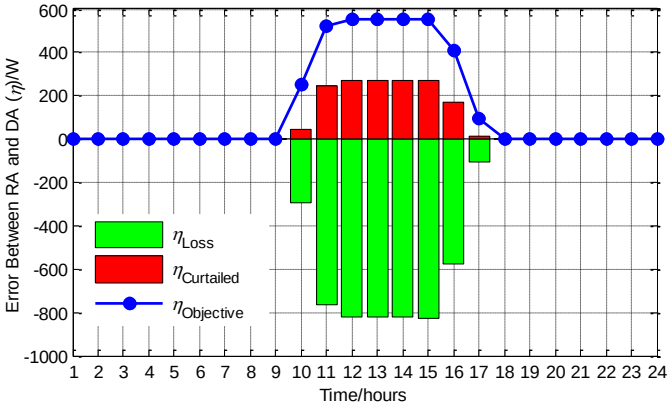

Fig. 6. Error in network losses, curtailed active power and optimal objective value between DA and RA.

For the case with the uncertainty level being 20% and the budget factor of PV systems for ancillary services being K=5, the traditional method DA and the proposed approach RA are compared in Fig. 5. Therein, Fig. 5 shows that the results of the optimal selection of PV systems for ancillary services by the RA and DA approaches are different. Moreover, it is interesting to find that the #5 and #15 PV systems are always selected during the daytime by the DA scheme, while the #2, #3, #7, #9 and #17 PV systems are always out of selection by both methods. This implies that the #5 and #15 PV systems are critical for improving the condition of active distribution network considering PV uncertainties.

Moreover, the errors in network losses (η_{Loss}), curtailed active power ($\eta_{\mathrm{Curtailed}}$) and optimal objective value ($\eta_{\mathrm{Objective}}$) between the RA and DA approaches are depicted in Fig. 6, which shows that during 1:00~5:00 a.m. and 21:00~24:00p.m., there is no uncertain power generation. Thus, both methods give the same optimal selection. During 6:00~9:00 a.m. and 18:00~20:00 p.m., when the power generation is relatively small, the RA and DA approaches also give the same optimal selection, leading to zero errors of η_{Loss}, $\eta_{\mathrm{Curtailed}}$ and $\eta_{\mathrm{Objective}}$. In contrast, during 10:00 a.m. ~ 17:00 p.m., the power generation is large and the uncertainties have a significant impact on the results of the two methods. Consequently, the RA can achieve less network losses than the worst case of the DA, but it results

This article has been accepted for publication in a future issue of this journal, but has not been fully edited. Content may change prior to final publication. Citation information: DOI 10.1109/TSTE.2016.2605926, IEEE Transactions on Sustainable Energy

in more curtailment of PV power. Notably, the total reduction of network losses by the RA is much more than the loss of PV generation. As a result, the optimal objective value by the RA is much better than that of the worst case of DA. This implies that the proposed robust optimization RA can achieve better performance than what the DA does.

Furthermore, the curtailed power and voltage magnitude in active distribution network over 24 hours are shown in Fig. 7 and Fig. 8. Here, we set the voltage magnitude limit to be within [0.95, 1.05] p.u.. During 10:00 a.m.~17:00 p.m., the solar irradiation is strong and the power flow becomes reverse, so voltage magnitudes at the PV system buses increase along with the PV generation units to the upper bound (1.05 p.u.). Meanwhile, the network losses will also increase due to the high penetration of PV systems. However, the optimal dispatch of PV inverters allows curtailing PV generation and absorbing more reactive power to alleviate the violation of the voltage magnitude and reduce the total network losses, so that the total real power surplus is maximized.

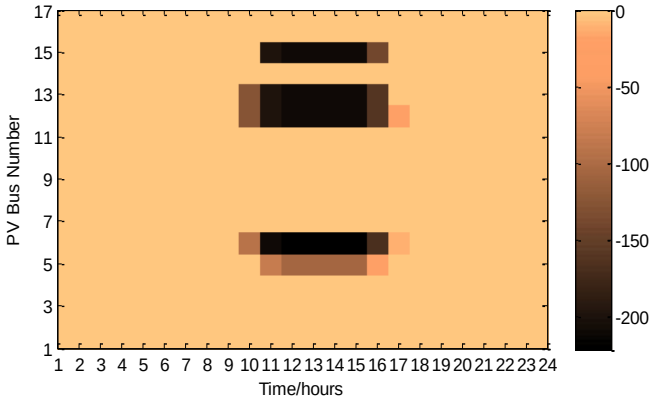

Fig. 7. Curtailed power in active distribution network over 24 hours.

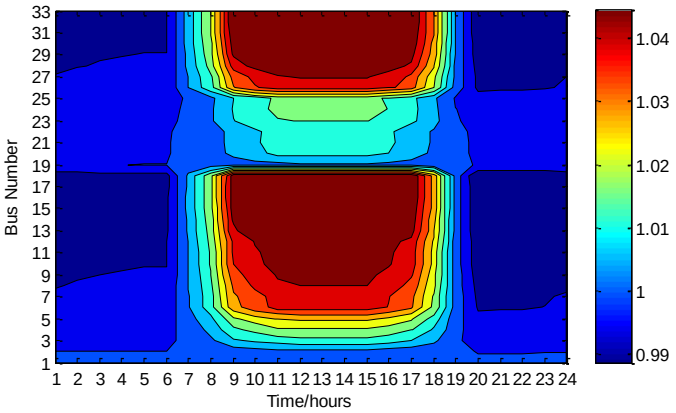

Fig. 8. Voltage magnitude in active distribution network over 24 hours.

In addition, impacts of the budget factor K and uncertainty α on the error η between the proposed RA and the worst case of the DA are shown in Fig. 9 and Fig. 10. The results imply that, by increasing either the budget factor K or the uncertainty α, more network losses will be reduced (i.e., η_{Loss} decreases) in the case of the RA, whereas more PV generation will be curtailed (i.e., $\eta_{\text{Curtailed}}$ increases). However, the total real power surplus $\eta_{\text{Objective}}$ is also increasing, which illustrates that the RA method attains better optimal value than the worst case of DA especially for larger uncertainties and budget factors. Obviously, a larger budget factor K means that there are more PV systems participating in ancillary services, which gives a rise to enough reactive power control and improves the system condition.

In particular, it is interesting to find that when $0 \le K \le 5$, $\eta_{\text{Objective}}$ is increased significantly with the increase of the budget factor K, whereas when $K \ge 6$, $\eta_{\text{Objective}}$ only increases slightly with the increase of the budget factor K. This suggests that the robust optimization needs only a fraction of PV systems to participate into ancillary services to achieve a majority of benefits (i.e., total real power surplus) comparing to the worst case of the DA. Moreover, more benefits will be obtained from the robust optimization under larger uncertainties.

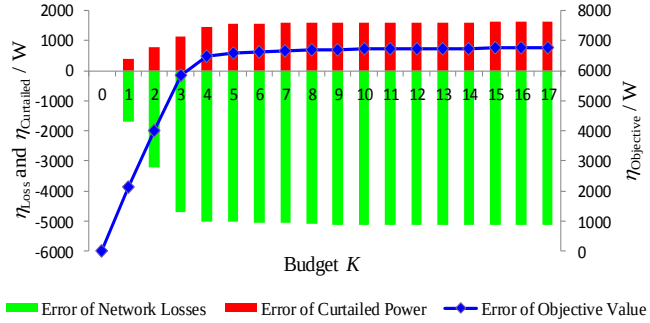

Fig. 9. Impact of the budget factor K on the error η.

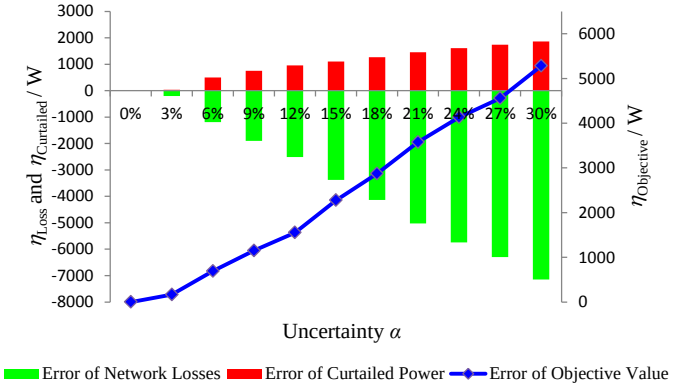

Fig. 10. Impact of the uncertainty α on the error η.

B. 123-bus Test System

For this test system, the topology is shown in Fig. 11, where 20 PV bases are considered with the capacity of each PV base being 300 kW. The factor of load and PV output curve in Fig. 4 is also adopted. Since the location of PV arrays may have an impact on the optimization results, two configurations are thus studied for comparison. In the first configuration, the PV arrays are connected to the buses {2, 5, 6, 9, 10, 13, 33, 35, 40, 55, 66, 78, 91, 92, 106, 121, 119, 118, 104, 107} and in the other configuration, the PV arrays are connected to the buses {5, 16, 29, 33, 46, 43, 41, 59, 96, 92, 90, 88, 64, 83, 79, 75, 71, 118, 104, 107}.

This article has been accepted for publication in a future issue of this journal, but has not been fully edited. Content may change prior to final publication. Citation information: DOI 10.1109/TSTE.2016.2605926, IEEE Transactions on Sustainable Energy

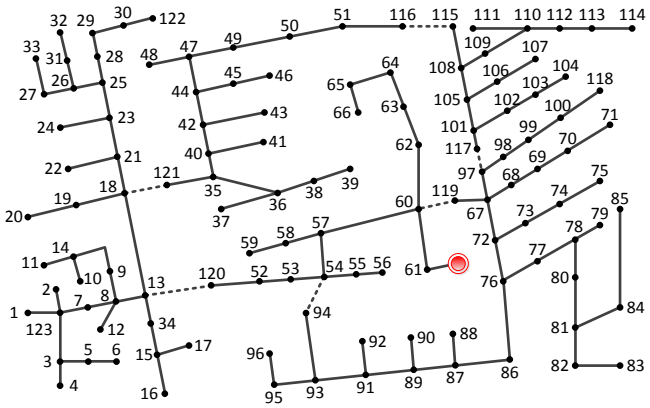

Fig. 11. A 123-bus radial network topology.

For the case with the uncertainty level being 20% and the budget factor of PV systems for ancillary services being K=5, the results on the two configurations by the proposed robust optimization approach are compared in Fig. 12 and Fig. 13. It can be observed in Fig. 12 that PV systems at bus #5 and #118 are selected for the first configuration, whereas neither is utilized for the second configuration. This implies that the location of PV arrays affects the selection of the critical PV inverters for providing ancillary services.

Meanwhile, the impacts of the budget factor K on the error η for the two configurations are shown in Fig. 14 and Fig. 15. Similar results as in the 33-bus system can be observed that, an increase in the budget factor K will result in that more network losses will be reduced (i.e., η_{Loss} decreases). Thus, more PV generation will be curtailed (i.e., $\eta_{\text{Curtailed}}$ increases). To sum up, the total real power surplus $\eta_{\text{Objective}}$ increases as a result. However, for the first configuration, when $0 \le K \le 5$, $\eta_{\text{Objective}}$ increases significantly; whilst $K \ge 6$, $\eta_{\text{Objective}}$ only increases slightly along with the increase of the budget factor K. In contrast, for the second configuration, the threshold of the budget factor K is 7. That is to say, when $0 \le K \le 7$, $\eta_{\text{Objective}}$ has a substantial increase; while $K \ge 7$, $\eta_{\text{Objective}}$ only increases slightly along with the budget factor increase. Moreover, when comparing Fig. 12 and Fig. 13, it can be found that:

1) For the same budget factor K, η_{Loss} of the first configuration is smaller than that of the second configuration;
2) $\eta_{\text{Curtailed}}$ of the first configuration is larger than that of the second configuration; and
3) $\eta_{\text{Objective}}$ of the first configuration is larger than that of the second configuration.

This implies that the location of PV arrays will affect the optimal number of the selected critical PV inverters for providing ancillary services as well as the value of network losses and curtailed PV power.

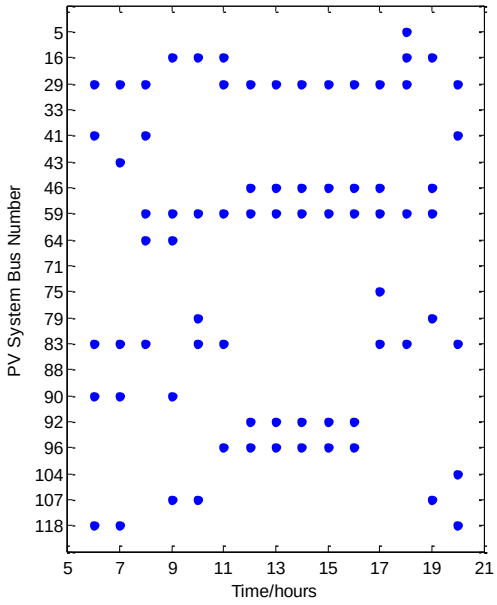

Fig. 12. Optimal selection of the PV systems for the first configuration.

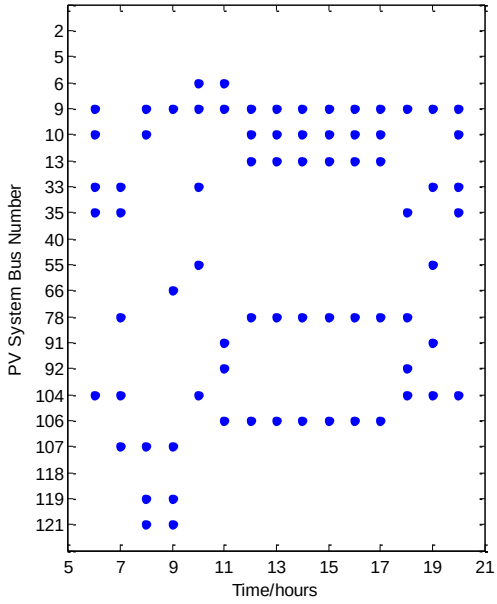

Fig. 13. Optimal selection of the PV systems for the second configuration.

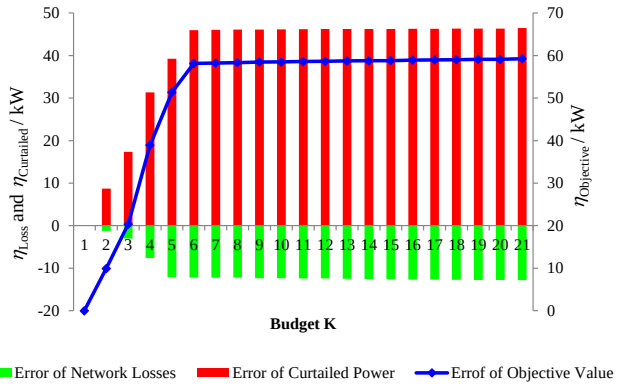

Fig. 14. Impact of the budget factor K on the error η for the first configuration.

This article has been accepted for publication in a future issue of this journal, but has not been fully edited. Content may change prior to final publication. Citation information: DOI 10.1109/TSTE.2016.2605926, IEEE Transactions on Sustainable Energy

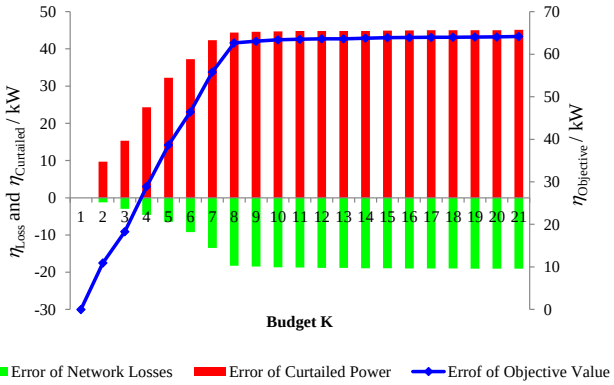

Fig. 15. Impact of the budget factor K on the error η for the second configuration.

V. Conclusions

A two-stage robust optimal inverter dispatch model to address the uncertainties of PV generation in active distribution networks has been proposed. The proposed solution aims to find a robust optimal solution while satisfying all the constraints under any possible realization within the uncertain PV power output. Then, a mixed integer second order cone programming model is set up with respect to the conic relaxation based branch flow formulation. Furthermore, a new column-and-constraint generation algorithm is utilized to solve the proposed two-stage robust optimal inverter dispatch model based on second order cone programming. The comparison with the deterministic approach on a 33-bus test system shows that the robust optimization approach can obtain much better optimal value under the worst case than the deterministic approach with the consideration of the uncertainties in PV system power generation. Moreover, more benefits will be obtained from the robust optimization under even larger uncertainty conditions.

Finally, the proposed two-stage robust optimal inverter dispatch model has been designed for selecting the optimal subset of PV inverters against the uncertainties in PV generation output in the day-ahead operation. The results can provide optimal strategy for the PV customers who want to participate into ancillary services. Moreover, the framework of the proposed second-order cone programming based column-and-constraint generation algorithm is a general method for the AC power flow based robust optimization, which can be extended to other applications in the distribution networks.

References

[1] S. Junseok, V. Krishnamurthy; A. Kwasinski; R. Sharma, "Development of a markov-chain-based energy storage model for power supply availability assessment of photovoltaic generation plants," *IEEE Transactions on Sustainable Energy*, vol.4, no.2, pp.491-500, 2013.

[2] M.Z.S. El-Dein, M. Kazerani, M.M.A. Salama, "'Optimal photovoltaic array reconfiguration to reduce partial shading losses," *IEEE Transactions on Sustainable Energy* , vol.4, no.1, pp.145-153, 2013.

[3] K. Touafek, M. Haddadi, A. Malek, "Modeling and experimental validation of a new hybrid photovoltaic thermal collector," *IEEE* Transactions *on Energy Conversion*, vol.26, no.1, pp.176-183, 2011.

[4] C.V. Nayar, M. Ashari, W.W.L. Keerthipala, "A grid-interactive photovoltaic uninterruptible power supply system using battery storage and a back up diesel generator," *IEEE Transactions on Energy Conversion*, vol.15, no.3, pp.348-353, 2000.

[5] BP, BP Statistical Review of World Energy, June 2015, available at :http://www.bp.com/content/dam/bp/pdf/energy-conomics/statistical-review-2015/bp-statistical-review-of-world-energy-2015-full-report.pdf

[6] C. Rodriguez and J. D. K. Bishop, "Organic architecture for small- to large-scale photovoltaic power stations,"*IEEE Transactions on Industrial Electronics*, vol. 56, no. 11, pp. 4332-4343, 2009.

[7] Y. Riffonneau, S. Bacha, F. Barruel, S. Ploix, "Optimal power flow management for grid connected pv systems with batteries," *IEEE Transactions on Sustainable Energy* , vol.2, no.3, pp.309-320, 2011

[8] Honrubia-Escribano, T. García-Sánchez, E. Gómez-Lázaro, et al, "Power quality surveys of photovoltaic power plants: characterisation and analysis of grid-code requirements,"*IET Renewable Power Generation*, vol. 9, no. 5, pp. 466-473, 2015.

[9] N. Saadat, S. S. Choi, D. M. Vilathgamuwa, "A series-connected photovoltaic distributed generator capable of enhancing power quality," *IEEE Trans. on Energy Conversion*, vol. 28, no. 4, pp. 1026-1035, 2015.

[10] F. Cardoso Melo, R. Ruiz Spaduto, L. C. Gomes de Freitas, C. E. Tavares, J.R. Macedo, P.H. Oliveria Rezende, "Harmonic distortion analysis in a low voltage grid-connected photovoltaic system," *Latin America Transactions, IEEE*, vol.13, no.1, pp.136-142, 2015.

[11] M. I. Hamid, A. Jusoh, M. Anwari, "Photovoltaic plant with reduced output current harmonics using generation-side active power conditioner,"*IET Renew. Power Gen.*, vol. 8, no. 7, pp. 817 - 826, 2014.

[12] Y. H. Hu; Y. Du; W. D. Xiao, et al, "DC-link voltage control strategy for reducing capacitance and total harmonic distortion in single-phase grid-connected photovoltaic inverters," *IET Power Electronics*, vol. 8, no. 8, pp. 1386-1393, 2015.

[13] M. Castilla, J. Miret, A. Camacho, J. Matas, L.G. de Vicuna, , "Reduction of current harmonic distortion in three-phase grid-connected photovoltaic inverters via resonant current control," *IEEE Transactions on Industrial Electronics*, vol.60, no.4, pp.1464-1472, 2013.

[14] W. Xiao, W. G. Dunford, P. R. Palmer, A. Capel, "Regulation of photovoltaic voltage," *IEEE Transactions on Industrial Electronics*, vol.54, no.3, pp.1365-1374, 2007.

[15] Yuzuru Ueda, K. Kurokawa, T. Tanabe, K. Kitamura, H. Sugihara, "Analysis results of output power loss due to the grid voltage rise in grid-connected photovoltaic power generation systems," *IEEE Transactions on Industrial Electronics*, vol.55, no.7, pp.2744-2751, 2008 .

[16] G. Mokhtari, A. Ghosh, G. Nourbakhsh, G. Ledwich, "Smart robust resources control in LV network to deal with voltage rise issue," *IEEE Transactions on Sustainable Energy*, vol.4, no.4, pp.1043-1050, 2013.

[17] T. Stetz, F. Marten, M. Braun, "Improved low voltage grid-integration of photovoltaic systems in germany," *IEEE Transactions on Sustainable Energy*, vol.4, no.2, pp.534-542, 2013.

[18] P. Jahangiri, D.C. Aliprantis, "Distributed volt/var control by PV inverters," *IEEE Trans. on Power Systems*, vol.28, no.3, pp.3429-3439, 2013.

[19] R. Tonkoski, L. A. C. Lopes, T. H. M. El-Fouly, "Coordinated active power curtailment of grid connected PV inverters for overvoltage prevention,"*IEEE Trans. Sustain. Energy*, vol. 2, no. 2, pp. 139-147, 2011.

[20] R. Tonkoski and L. A. C. Lopes, "Impact of active power curtailment on overvoltage prevention and energy production of PV inverters connected to low voltage residential feeders," *Renew. Energy*, vol. 36, no. 12, pp. 3566-3574, 2011.

[21] E. Dall'Anese, S.V. Dhople, G.B. Giannakis, "Optimal dispatch of photovoltaic inverters in residential distribution systems,", *IEEE Transactions on Sustainable Energy*, vol.5, no.2, pp.487-497, 2014.

[22] E. Dall'Anese, S.V. Dhople, B.B. Johnson, G.B. Giannakis, "Decentralized optimal dispatch of photovoltaic inverters in residential distribution systems," *IEEE Journal of Photovoltaics*, vol.5, no.1, pp.350-359, 2015.

[23] E. Dall'Anese, S.V. Dhople, B. B. Johnson, G. B. Giannakis, "Optimal dispatch of residential photovoltaic inverters under forecasting uncertainties," *IEEE Trans. on Energy Conv.*, vol. 29, no. 4, pp.957-967, 2014.

[24] E. Chiodo, D. Lauria, C. Pisani, "Availability analysis of photovoltaic inverters in presence of uncertain data via Bayesian approach," *IET Gen., Transm. & Distrib.*, vol. 9, no. 13, pp. 1681-1687, 2015.

[25] A. Tuohy, J. Zack, S.E. Haupt, J. Sharp, M. Ahlstrom, S. Dise, E. Grimit, C. Mohrlen, M. Lange, M. Garcia Casado, J. Black, M. Marquis, C.

Collier, "Solar forecasting: methods, challenges, and performance," *Power and Energy Magazine, IEEE* , vol.13, no.6, pp.50-59, 2015.

[26] S. Talari, M. Yazdaninejad, M.-R. Haghifam, "Stochastic-based scheduling of the microgrid operation including wind turbines, photovoltaic cells, energy storages and responsive loads," *Generation, Transmission & Distribution, IET* , vol.9, no.12, pp.1498-1509, 2015.

[27] Y. P. Agalgaonkar, B. C. Pal, R. A. Jabr, "Stochastic distribution system operation considering voltage regulation risks in the presence of PV generation," *IEEE Transactions on Sustainable Energy*, vol.6, no.4, pp.1315-1324, 2015.

[28] H. Xin, Y. Liu, Z. Qu and et al., "Distributed control and generation estimation method for integrating high-density photovoltaic systems," *IEEE Trans. on Energy Conv.*, vol.29, no.4, pp.988-996, 2014.

[29] A. Arabali, M. Ghofrani, M. Etezadi-Amoli, M.S. Fadali, "Stochastic performance assessment and sizing for a hybrid power system of solar/wind/energy storage," *IEEE Transactions on Sustainable Energy*, vol.5, no.2, pp.363-371, 2014.

[30] A. Ben-Tal and A. Nemirovski, "Robust optimization–methodology and applications,"*Mathematical Prog.*, vol. 92, no. 3, pp. 453-480, 2002.

[31] H. G. Beyer and B. Sendhoff, "Robust optimization–a comprehensive survey,"*Computer methods in applied mechanics and engineering*, vol. 196, no. 33, pp. 3190-3218, 2007.

[32] A. Ben-Tal, L. El Ghaoui and A. Nemirovski, "Robust optimization,"*Princeton University Press*, 2009.

[33] M. E. Baran, F. F. Wu, "Optimal sizing of capacitors placed on a radial distribution system," *IEEE Trans. on Power Del.*, vol.4, no.1, pp.735-743, 1989.

[34] T. Ding, R. Bo, W. Gu, H. Sun, "Big-M Based MIQP Method for Economic Dispatch With Disjoint Prohibited Zones," *IEEE Trans. Power Syst.*, vol. 29, no. 2, pp. 976–977, 2014.

[35] T. Ding, R. Bo, F. Li and et al., "A bi-level branch and bound method for economic dispatch with disjoint prohibited zones considering network losses," *IEEE Trans. on Power Sys.*, vol.30, no.6, pp.2841-2855, 2015.

[36] B. Zeng, and L. Zhao, "Solving two-stage robust optimization problems using a column-and-constraint generation method," *Operations Research Letters*, vol. 41, no. 5, pp. 457-461, 2013.

[37] R. Jiang, J. Wang, M. Zhang, and Y. Guan, "Two-stage minimax regret unit commitment considering wind power uncertainty," *IEEE Trans. Power Syst*., vol. 28, no. 3, pp. 2271–2282, Aug. 2013.

[38] T. Ding, S. Liu and W. Yuan and et al., "A two-stage robust reactive power optimization considering uncertain wind power integration in active distribution networks," *IEEE Trans. on Sustainable Energy*, vol. 7, no. 1, pp. 301-311, 2016.

[39] T. Ding, F. Li, X. Li, and et al, "Interval radial power flow using extended Distflow formulation and Krawczyk iteration method with sparse approximate inverse preconditioner," *IET Generation Transmission & Distribution*, vol. 9, no. 14, pp. 1998-2006, 2015.

Tao Ding (S'13–M'15) received the B.S.E.E. and M.S.E.E. degrees from Southeast University, Nanjing, China, in 2009 and 2012, respectively, and the Ph.D. degree from Tsinghua University, Beijing, China, in 2015. During 2013~2014, he was a visiting scholar with the Department of Electrical Engineering and Computer Science, The University of Tennessee, Knoxville (UTK), TN, USA. He received the excellent master and doctoral dissertation from Southeast University and Tsinghua University, respectively, and outstanding graduate award of Beijing City. Dr. Ding has published more than 60 technical papers and authored by "Springer Theses" recognizing outstanding Ph.D. research around the world and across the physical sciences – *Power System Operation with Large Scale Stochastic Wind Power Integration*.

He is currently an associate professor in the State Key Laboratory of Electrical Insulation and Power Equipment, the School of Electrical Engineering, Xi'an Jiaotong University. His current research interests include electricity markets, power system economics and optimization methods, and power system planning and reliability evaluation.

Cheng Li received the B.S. degree from the School of Electrical Engineering, Xi'an Jiaotong University, Xi'an, China, in 2016. He is currently pursuing the M.S. degree at Xi'an Jiaotong University. His major research interests include power system optimization and renewable energy integration.

Yongheng Yang (S'12 - M'15) received the B.Eng. degree in 2009 from Northwestern Polytechnical University, China and the Ph.D. degree in 2014 from Aalborg University, Denmark.

He was a postgraduate with Southeast University, China, from 2009 to 2011. In 2013, he was a Visiting Scholar with Texas A&M University, USA. Since 2014, he has been with the Department of Energy Technology, Aalborg University, where currently he is an Assistant Professor. His research interests are focused on grid integration of renewable energy systems, power converter design, analysis and control, harmonics identification and mitigation, and reliability in power electronics. Dr. Yang has published more than 80 technical papers and co-authored a book – *Periodic Control of Power Electronic Converters* (London, UK: IET, 2017).

Dr. Yang is a Member of the IEEE Power Electronics Society (PELS) Students and Young Professionals Committee, where he serves as the Global Strategy Chair and responsible for the IEEE PELS Students and Young Professionals Activities. He served as a Guest Associate Editor of **IEEE JOURNAL OF EMERGING AND SELECTED TOPICS IN POWER ELECTRONICS**, and has also been invited as a Guest Editor of *Applied Sciences*. He is an active reviewer for relevant top-tier journals.

Jiangfeng Jiang received the B.S. degree from the School of Electrical Engin eering, Xi'an Jiaotong University, Xi'an, China, in 2014. He is currently pursu ing the Ph.D degree at Xi'an Jiaotong University. His major research interests include power system optimization and Load forecasting.

Zhaohong Bie (M'98–SM'12) received the B.S. and M.S. degrees from the Electric Power Department of Shandong University, Jinan, China, in 1992 and 1994, respectively, and the Ph.D. degree from Xi'an Jiaotong University, Xi'an, China, in 1998. Currently, she is a Professor in the State Key Laboratory of Electrical Insulation and Power Equipment and the School of Electrical Engineering, Xi'an Jiaotong University. Her main interests are power system planning and reliability evaluation, as well as the integration of the renewable energy.

Frede Blaabjerg (S'86 - M'88 - SM'97 - F'03) was with ABB-Scandia, Randers, Denmark, from 1987 to 1988. From 1988 to 1992, he was a Ph.D. Student with Aalborg University, Aalborg, Denmark. He became an Assistant Professor in 1992, an Associate Professor in 1996, and a Full Professor of power electronics and drives in 1998 at Aalborg University. His current research interests include power electronics and its applications such as in wind turbines, PV systems, reliability, harmonics and adjustable speed drives.

Prof. Blaabjerg has received 17 IEEE Prize Paper Awards, the IEEE Power Electronics Society (PELS) Distinguished Service Award in 2009, the EPE-PEMC Council Award in 2010, the IEEE William E. Newell Power Electronics Award in 2014 and the Villum Kann Rasmussen Research Award in 2014. He was an Editor-in-Chief of the **IEEE TRANSACTIONS ON POWER ELECTRONICS** from 2006 to 2012. Prof. Blaabjerg was nominated in 2014 and 2015 by Thomson Reuters to be between the most 250 cited researchers in Engineering in the world.